EUROPEAN ORGANISATION FOR NUCLEAR RESEARCH

CERN-PPE/96-068
23 May 1996

A First Measurement of the $\Lambda\bar{\Lambda}$ and $\Lambda\Lambda$ ($\bar{\Lambda}\bar{\Lambda}$) Spin Compositions in Hadronic Z^0 Decays

The OPAL Collaboration

Abstract

The spin composition of $\Lambda\bar{\Lambda}$, $\Lambda\Lambda$ and $\bar{\Lambda}\bar{\Lambda}$ pairs at low invariant mass values has been measured for the first time in multihadronic Z^0 decays with the OPAL detector at LEP. No single spin state has been observed in the $\Lambda\bar{\Lambda}$ sample, verifying that the low mass enhancement in this sample, attributed to local baryon number compensation, is not a resonance state. The fraction of the spin 1 contribution to the $\Lambda\bar{\Lambda}$ pairs was found to be consistent with the value 0.75, as expected from a statistical spin mixture. This may be the net effect of many different QCD processes which contribute to the hyperon anti-hyperon pair production. The spin composition of the identical $\Lambda\Lambda$ and $\bar{\Lambda}\bar{\Lambda}$ pairs, well above threshold, is found to be similar to that of the $\Lambda\bar{\Lambda}$ sample. A $\Lambda\Lambda$ emitter dimension is estimated from the data assuming the onset of the Pauli exclusion principle near threshold.

(To be submitted to Physics Letters B)

The OPAL Collaboration

G. Alexander[23], J. Allison[16], N. Altekamp[5], K. Ametewee[25], K.J. Anderson[9], S. Anderson[12], S. Arcelli[2], S. Asai[24], D. Axen[29], G. Azuelos[18,a], A.H. Ball[17], E. Barberio[26], R.J. Barlow[16], R. Bartoldus[3], J.R. Batley[5], G. Beaudoin[18], J. Bechtluft[14], C. Beeston[16], T. Behnke[8], A.N. Bell[1], K.W. Bell[20], G. Bella[23], S. Bentvelsen[8], P. Berlich[10], S. Bethke[14], O. Biebel[14], V. Blobel[8], I.J. Bloodworth[1], J.E. Bloomer[1], P. Bock[11], H.M. Bosch[11], M. Boutemeur[18], B.T. Bouwens[12], S. Braibant[12], R.M. Brown[20], H.J. Burckhart[8], C. Burgard[27], R. Bürgin[10], P. Capiluppi[2], R.K. Carnegie[6], A.A. Carter[13], J.R. Carter[5], C.Y. Chang[17], C. Charlesworth[6], D.G. Charlton[1,b], D. Chrisman[4], S.L. Chu[4], P.E.L. Clarke[15], I. Cohen[23], J.E. Conboy[15], O.C. Cooke[16], M. Cuffiani[2], S. Dado[22], C. Dallapiccola[17], G.M. Dallavalle[2], S. De Jong[12], L.A. del Pozo[8], K. Desch[3], M.S. Dixit[7], E. do Couto e Silva[12], M. Doucet[18], E. Duchovni[26], G. Duckeck[8], I.P. Duerdoth[16], J.E.G. Edwards[16], P.G. Estabrooks[6], H.G. Evans[9], M. Evans[13], F. Fabbri[2], P. Fath[11], F. Fiedler[12], M. Fierro[2], H.M. Fischer[3], R. Folman[26], D.G. Fong[17], M. Foucher[17], H. Fukui[24], A. Fürtjes[8], P. Gagnon[7], A. Gaidot[21], J.W. Gary[4], J. Gascon[18], S.M. Gascon-Shotkin[17], N.I. Geddes[20], C. Geich-Gimbel[3], F.X. Gentit[21], T. Geralis[20], G. Giacomelli[2], P. Giacomelli[4], R. Giacomelli[2], V. Gibson[5], W.R. Gibson[13], D.M. Gingrich[30,a], J. Goldberg[22], M.J. Goodrick[5], W. Gorn[4], C. Grandi[2], E. Gross[26], M. Gruwé[8], C. Hajdu[32], G.G. Hanson[12], M. Hansroul[8], M. Hapke[13], C.K. Hargrove[7], P.A. Hart[9], C. Hartmann[3], M. Hauschild[8], C.M. Hawkes[5], R. Hawkings[8], R.J. Hemingway[6], G. Herten[10], R.D. Heuer[8], M.D. Hildreth[8], J.C. Hill[5], S.J. Hillier[1], T. Hilse[10], J. Hoare[5], P.R. Hobson[25], R.J. Homer[1], A.K. Honma[28,a], D. Horváth[32,c], R. Howard[29], R.E. Hughes-Jones[16], D.E. Hutchcroft[5], P. Igo-Kemenes[11], D.C. Imrie[25], M.R. Ingram[16], A. Jawahery[17], P.W. Jeffreys[20], H. Jeremie[18], M. Jimack[1], A. Joly[18], C.R. Jones[5], G. Jones[16], M. Jones[6], R.W.L. Jones[8], U. Jost[11], P. Jovanovic[1], T.R. Junk[8], D. Karlen[6], K. Kawagoe[24], T. Kawamoto[24], R.K. Keeler[28], R.G. Kellogg[17], B.W. Kennedy[20], B.J. King[8], J. Kirk[29], S. Kluth[8], T. Kobayashi[24], M. Kobel[10], D.S. Koetke[6], T.P. Kokott[3], S. Komamiya[24], R. Kowalewski[8], T. Kress[11], P. Krieger[6], J. von Krogh[11], P. Kyberd[13], G.D. Lafferty[16], H. Lafoux[21], R. Lahmann[17], W.P. Lai[19], D. Lanske[14], J. Lauber[15], S.R. Lautenschlager[31], J.G. Layter[4], D. Lazic[22], A.M. Lee[31], E. Lefebvre[18], D. Lellouch[26], J. Letts[2], L. Levinson[26], C. Lewis[15], S.L. Lloyd[13], F.K. Loebinger[16], G.D. Long[17], M.J. Losty[7], J. Ludwig[10], A. Luig[10], A. Malik[21], M. Mannelli[8], S. Marcellini[2], C. Markus[3], A.J. Martin[13], J.P. Martin[18], G. Martinez[17], T. Mashimo[24], W. Matthews[25], P. Mättig[3], W.J. McDonald[30], J. McKenna[29], E.A. Mckigney[15], T.J. McMahon[1], A.I. McNab[13], R.A. McPherson[8], F. Meijers[8], S. Menke[3], F.S. Merritt[9], H. Mes[7], J. Meyer[27], A. Michelini[2], G. Mikenberg[26], D.J. Miller[15], R. Mir[26], W. Mohr[10], A. Montanari[2], T. Mori[24], M. Morii[24], U. Müller[3], H.A. Neal[8], B. Nellen[3], B. Nijjhar[16], R. Nisius[8], S.W. O'Neale[1], F.G. Oakham[7], F. Odorici[2], H.O. Ogren[12], T. Omori[24], M.J. Oreglia[9], S. Orito[24], J. Pálinkás[33,d], J.P. Pansart[21], G. Pásztor[32], J.R. Pater[16], G.N. Patrick[20], M.J. Pearce[1], S. Petzold[27], P. Pfeifenschneider[14], J.E. Pilcher[9], J. Pinfold[30], D.E. Plane[8], P. Poffenberger[28], B. Poli[2], A. Posthaus[3], H. Przysiezniak[30], D.L. Rees[1], D. Rigby[1], S.A. Robins[13], N. Rodning[30], J.M. Roney[28], A. Rooke[15], E. Ros[8], A.M. Rossi[2], M. Rosvick[28], P. Routenburg[30], Y. Rozen[8], K. Runge[10], O. Runolfsson[8], U. Ruppel[14], D.R. Rust[12], R. Rylko[25], E.K.G. Sarkisyan[23], M. Sasaki[24], C. Sbarra[2], A.D. Schaile[8,e], O. Schaile[10], F. Scharf[3], P. Scharff-Hansen[8], P. Schenk[4], B. Schmitt[3], S. Schmitt[11], M. Schröder[8], H.C. Schultz-Coulon[10], M. Schulz[8], P. Schütz[3], W.G. Scott[20], T.G. Shears[16], B.C. Shen[4], C.H. Shepherd-Themistocleous[27], P. Sherwood[15], G.P. Siroli[2], A. Sittler[27], A. Skillman[15], A. Skuja[17], A.M. Smith[8], T.J. Smith[28], G.A. Snow[17], R. Sobie[28], S. Söldner-Rembold[10], R.W. Springer[30], M. Sproston[20], A. Stahl[3], M. Starks[12], M. Steiert[11], K. Stephens[16], J. Steuerer[27], B. Stockhausen[3], D. Strom[19], F. Strumia[8], P. Szymanski[20], R. Tafirout[18], S.D. Talbot[1], S. Tanaka[24], P. Taras[18], S. Tarem[22], M. Tecchio[8], M. Thiergen[10], M.A. Thomson[8], E. von Törne[3], S. Towers[6], M. Tscheulin[10], T. Tsukamoto[24], E. Tsur[23], A.S. Turcot[9], M.F. Turner-Watson[8], P. Utzat[11], R. Van Kooten[12], G. Vasseur[21], M. Verzocchi[10], P. Vikas[18], M. Vincter[28], E.H. Vokurka[16], F. Wäckerle[10],

A. Wagner[27], C.P. Ward[5], D.R. Ward[5], J.J. Ward[15], P.M. Watkins[1], A.T. Watson[1], N.K. Watson[7], P. Weber[6], P.S. Wells[8], N. Wermes[3], J.S. White[28], B. Wilkens[10], G.W. Wilson[27], J.A. Wilson[1], T. Wlodek[26], G. Wolf[26], S. Wotton[5], T.R. Wyatt[16], S. Yamashita[24], G. Yekutieli[26], V. Zacek[18],

[1]School of Physics and Space Research, University of Birmingham, Birmingham B15 2TT, UK
[2]Dipartimento di Fisica dell' Università di Bologna and INFN, I-40126 Bologna, Italy
[3]Physikalisches Institut, Universität Bonn, D-53115 Bonn, Germany
[4]Department of Physics, University of California, Riverside CA 92521, USA
[5]Cavendish Laboratory, Cambridge CB3 0HE, UK
[6] Ottawa-Carleton Institute for Physics, Department of Physics, Carleton University, Ottawa, Ontario K1S 5B6, Canada
[7]Centre for Research in Particle Physics, Carleton University, Ottawa, Ontario K1S 5B6, Canada
[8]CERN, European Organisation for Particle Physics, CH-1211 Geneva 23, Switzerland
[9]Enrico Fermi Institute and Department of Physics, University of Chicago, Chicago IL 60637, USA
[10]Fakultät für Physik, Albert Ludwigs Universität, D-79104 Freiburg, Germany
[11]Physikalisches Institut, Universität Heidelberg, D-69120 Heidelberg, Germany
[12]Indiana University, Department of Physics, Swain Hall West 117, Bloomington IN 47405, USA
[13]Queen Mary and Westfield College, University of London, London E1 4NS, UK
[14]Technische Hochschule Aachen, III Physikalisches Institut, Sommerfeldstrasse 26-28, D-52056 Aachen, Germany
[15]University College London, London WC1E 6BT, UK
[16]Department of Physics, Schuster Laboratory, The University, Manchester M13 9PL, UK
[17]Department of Physics, University of Maryland, College Park, MD 20742, USA
[18]Laboratoire de Physique Nucléaire, Université de Montréal, Montréal, Quebec H3C 3J7, Canada
[19]University of Oregon, Department of Physics, Eugene OR 97403, USA
[20]Rutherford Appleton Laboratory, Chilton, Didcot, Oxfordshire OX11 0QX, UK
[21]CEA, DAPNIA/SPP, CE-Saclay, F-91191 Gif-sur-Yvette, France
[22]Department of Physics, Technion-Israel Institute of Technology, Haifa 32000, Israel
[23]Department of Physics and Astronomy, Tel Aviv University, Tel Aviv 69978, Israel
[24]International Centre for Elementary Particle Physics and Department of Physics, University of Tokyo, Tokyo 113, and Kobe University, Kobe 657, Japan
[25]Brunel University, Uxbridge, Middlesex UB8 3PH, UK
[26]Particle Physics Department, Weizmann Institute of Science, Rehovot 76100, Israel
[27]Universität Hamburg/DESY, II Institut für Experimental Physik, Notkestrasse 85, D-22607 Hamburg, Germany
[28]University of Victoria, Department of Physics, P O Box 3055, Victoria BC V8W 3P6, Canada
[29]University of British Columbia, Department of Physics, Vancouver BC V6T 1Z1, Canada
[30]University of Alberta, Department of Physics, Edmonton AB T6G 2J1, Canada
[31]Duke University, Dept of Physics, Durham, NC 27708-0305, USA
[32]Research Institute for Particle and Nuclear Physics, H-1525 Budapest, P O Box 49, Hungary
[33]Institute of Nuclear Research, H-4001 Debrecen, P O Box 51, Hungary

[a] and at TRIUMF, Vancouver, Canada V6T 2A3
[b] and Royal Society University Research Fellow
[c] and Institute of Nuclear Research, Debrecen, Hungary
[d] and Department of Experimental Physics, Lajos Kossuth University, Debrecen, Hungary
[e] and Ludwig-Maximilians-Universität, München, Germany

1 Introduction

The fragmentation and hadronisation processes in high energy particle interactions have been the subject of many QCD-based theoretical investigations [1]. These theoretical models predict general features of multihadron states, such as the jet structure and the inclusive particle momentum spectrum, which have been confronted with the experimental findings. Additional information concerning the hadronisation processes comes from correlation studies of pairs of particles. Among these are the study of the Bose-Einstein Correlations (BEC) of identical bosons, mainly identical pions. From these studies one is able to extract the dimension of the particle emitter. Recently a new approach to the description of the parton to hadron conversion has been proposed [2], which is applied to final state bosons. In this approach the BEC of identical pions form an integral part of the model so that the BEC experimental measurements can serve to extract the basic model parameters. The BEC have also been investigated in the framework of the Lund fragmentation model [3] and compared to experimental data.

When extending such models to include baryons in the final state, the BEC obviously are no longer applicable and other correlations should be considered in order to investigate the underlying baryon production processes. Among those of interest is the spin composition of the baryon anti-baryon ($B\overline{B}$) final states produced in the hadronisation process. For two spin 1/2 baryons the total spin, $\vec{S} = \vec{S_B} + \vec{S_{\overline{B}}}$, may be 0 or 1. Baryon anti-baryon pairs can be produced by several QCD processes in high energy reactions. If the $B\overline{B}$ pair production is for example dominated by a single gluon emission, in analogy to the 'colour octet' mechanism [4] which is applied to J/ψ and Υ production, then the S = 1 state may dominate over the S = 0 state due to the vector ($J^P = 1^-$) nature of the gluon. This will be the case only as long as the soft gluons, which are needed to balance the colour, do not disturb too much the quantum state of the di–baryon system. If however many other diagrams, like those involving several gluons or the so called 'popcorn' [5] mechanism, also contribute to $B\overline{B}$ pair production, then one may have a statistical–like spin composition where, due to the 2S+1 factor, the S = 1 fraction is three times larger than that of the S = 0.

The main interest in studying the spin composition of identical baryons as a function of their invariant mass stem from the possibility to observe the decrease of the S = 1 state contribution, due to the Pauli exclusion principle, as the di–baryon energy approaches threshold. This then can serve as a measure of the baryon emitter dimension [6] in analogy to that obtained from the BEC measurements of identical bosons.

Here we describe a spin correlation analysis of inclusive $\Lambda\bar{\Lambda}$, $\Lambda\Lambda$ and $\bar{\Lambda}\bar{\Lambda}$ pairs which is only dependent on the relative polarisation of the two hyperons. The analysis is based on multihadronic Z^0 decay data recorded by the OPAL detector during the years 1990 to 1994 corresponding to an integrated luminosity of 137 pb^{-1}. We estimate that in our event sample about 20% of the Λ's originate from weak decays of baryons, mainly Ξ hyperons [7], and the rest stems from strong interactions. In addition we have used in the analysis 7.1×10^6 JETSET7.3 and JETSET7.4 Monte Carlo [8] events with a full detector simulation [9]. The JETSET parameters were adapted to OPAL data [10]. These Monte Carlo samples do not include any spin effects in the Λ production and decay. The data are studied as a function of the variable Q, frequently used in the BEC studies of identical bosons, which is related to the di–Λ invariant mass, $M_{\Lambda\Lambda}$, through the expression $Q = \sqrt{M^2_{\Lambda\Lambda} - 4m^2_{\Lambda}}$ and is equal to zero at threshold.

In Section 2 we outline the method used for the spin composition measurement and in Section 3 we describe the procedure adopted to obtain the experimental data samples and evaluate their backgrounds. In Section 4 our results for the spin compositions are described, and finally in Section 5 a summary and conclusions are given.

2 The Method

In general it is very difficult to measure in high energy reactions the relative contributions of the S = 0 and the S = 1 states to a di–baryon (B_1B_2 or $B_1\overline{B}_2$) system such as a p$\bar{\text{p}}$ pair. However, a relatively simple experimental method has recently been proposed [6] for the measurement of the S = 0 and S = 1 contributions to a given system of two spin 1/2 weakly decaying hyperons, like $\Lambda\bar{\Lambda}$ and $\Lambda\Lambda$ pairs, which is independent of their relative angular momentum ℓ. A comprehensive description of this method can be found in reference [6], so here we will only outline in brief some of the aspects which are relevant to our analysis.

The spin composition measurement is based on the distribution dN/dy^*, in the di–hyperon centre of mass (CM) system, where y^* is the cosine of the angle between the two hyperons' decay protons, each measured in its parent hyperon rest frame. If α_B is the hyperon decay parameter arising from parity violation, then the decay angular distribution of each hyperon in its rest frame is of the form [11]

$$dN/d\cos\theta_p = 1 - \alpha_B \cdot \cos\theta_p$$

where θ_p is the angle of the proton direction relative to the polarisation axis of the hyperon. The Wigner-Eckart theorem [12] then gives a relation between the average value of y^* and the average $\cos\theta_p$ values:

$$\frac{< y^* >}{< \cos\theta_{p_1} >< \cos\theta_{p_2} >} = \begin{cases} -3 & \text{for S} = 0 \\ +1 & \text{for S} = 1 \end{cases}$$

where S is the spin state of the di–baryon system. For the case of interest here, $< y^* >$ can be calculated at the $\Lambda\Lambda$ threshold by using the well measured α_Λ value [13] of 0.642 ± 0.013. Due to the fact that the Λ is a spin 1/2 particle, the dN/dy^* distribution cannot have a y^* dependence higher than its first power, so that the average value $< y^* >$ uniquely determines the angular distribution. Using α_Λ and the fact that $\alpha_{\overline{\Lambda}} = -\alpha_\Lambda$, one is then able to derive the y^* angular distributions at the di–hyperon threshold energy[1]. Thus for the S = 0 and S = 1 $\Lambda\bar{\Lambda}$ states one gets

$$dN/dy^*|_{S=0} = 1 + \alpha_\Lambda^2 \cdot y^* \qquad \text{and} \qquad dN/dy^*|_{S=1} = 1 - \frac{\alpha_\Lambda^2}{3} \cdot y^* \tag{1}$$

whereas for the S = 0 and S =1 $\Lambda\Lambda$ and $\bar{\Lambda}\bar{\Lambda}$ identical hyperon states one obtains

$$dN/dy^*|_{S=0} = 1 - \alpha_\Lambda^2 \cdot y^* \qquad \text{and} \qquad dN/dy^*|_{S=1} = 1 + \frac{\alpha_\Lambda^2}{3} \cdot y^* \tag{2}$$

It should be noted that for $\ell = 0$, the S = 1 state of two identical spin 1/2 particles is forbidden by the Pauli exclusion principle. Even though these dN/dy^* distributions are derived for a di–hyperon system at threshold, they can still be used at higher, but not relativistic, di–hyperon CM energies provided that the nucleon decay products are transformed to their parent hyperon rest frame (see reference [6]). Therefore we have limited our analysis to Q values less than 2.5 GeV.

Using the above equations one can evaluate, for a given di–Λ data sample, the relative contributions of the S = 0 and S = 1 states by fitting the expression:

$$dN/dy^* = (1-\epsilon) \cdot dN/dy^*|_{S=0} + \epsilon \cdot dN/dy^*|_{S=1} \tag{3}$$

to the measured dN/dy^* distribution. The parameter ϵ is the fraction of the S = 1 state contribution to the di–hyperon system. For a statistical spin mixture ensemble, where each spin state probability is weighted by the factor 2S+1, ϵ is equal to 0.75 which corresponds to a constant dN/dy^* distribution.

[1] Note that at threshold the single hyperon CM system, where $< \cos\theta_p >$ is evaluated, is the same as that of the di–hyperon system.

3 Experimental setup and data selection

3.1 The OPAL detector

Details of the OPAL detector and its performance at the LEP e^+e^- collider are given elsewhere [14]. Here we will describe briefly only those detector components pertinent to the present analysis, namely the central tracking chambers.

The central tracking chambers consist of a precision vertex detector, a large jet chamber, and additional z-chambers surrounding the jet chamber. The vertex detector is a 1 m long, two-layer cylindrical drift chamber which surrounds the beam pipe[2]. The jet chamber has a length of 4 m and a diameter of 3.7 m. It is divided into 24 sectors in ϕ, each equipped with 159 sense wires parallel to the beam ensuring a large number of measured points even for particles emerging from a secondary vertex. The jet chamber also provides a measurement of the specific energy loss, dE/dx, of charged particles [15]. A resolution of 3–4% on dE/dx has been obtained, allowing particle identification over a large momentum range. The z-chambers, 4 m long, 50 cm wide and 59 mm thick, allow a precise measurement of the z-coordinate of the charged tracks. They cover polar angles from 44° to 136° and 94% of the azimuthal angular range. All the chambers are contained in a solenoid providing an axial magnetic field of 0.435 T. The combination of these chambers leads to a momentum resolution of $\sigma_{p_t}/p_t \approx \sqrt{(0.02)^2 + (0.0015 \cdot p_t)^2}$, where p_t in GeV/c is the transverse momentum with respect to the beam direction. The first term under the square root sign represents the contribution from multiple scattering [16].

3.2 Data Selection

Hadronic Z^0 decays were selected according to the number of charged tracks and the visible energy of the event, using the criteria described in Ref. [17]. In addition, events where the thrust axis lay close to the beam axis were rejected by requiring $|\cos\vartheta_{\rm thrust}| < 0.9$, where $\vartheta_{\rm thrust}$ is the polar angle of the thrust vector determined from charged tracks. The analysis was performed on data collected on and around the Z^0 peak. With the requirement that the jet and z-chambers were fully operational, a total of 3.3×10^6 Z^0 hadronic decay events satisfied these selection criteria. The Λ baryons were selected by reconstructing the decay $\Lambda \to p\pi$, applying an improved version of the selection described as method 1 in Ref. [7]. All pairs of tracks with opposite charge were examined and the higher momentum track was assigned to be the proton track. In addition, the measurement of dE/dx were required to be consistent with the p and π hypotheses. Intersection points of track pairs in the plane perpendicular to the beam axis were considered to be secondary vertex candidates if the following requirements were satisfied:

- the radial distance from the intersection point to the primary vertex had to be larger than 1 cm and smaller than 150 cm;
- the reconstructed momentum vector of the Λ candidate in the plane perpendicular to the beam axis had to point within 2° to the primary vertex;
- if the secondary vertex was reconstructed inside the jet chamber volume, the radius of the first jet chamber hit of each of the two tracks had to be less than 3 cm from the secondary vertex;
- if the secondary vertex was not reconstructed inside the jet chamber, the impact parameter transverse to the beam direction (d_0) of the pion with respect to the main vertex had to be larger than 3 mm and the d_0 of the proton track had to exceed 1 mm;

[2] A right-handed coordinate system is adopted by OPAL, where the x-axis points to the centre of the LEP ring, and positive z is along the electron beam direction. The angles θ and ϕ are the polar and azimuthal angles, respectively.

- photon conversions were rejected if the invariant mass of the track pair, assumed to be an e^+e^- pair, was smaller than 40 MeV;
- a mass window cut of $\pm$ 6 MeV, around our mean fitted Λ mass value of 1115.7 MeV, was applied. This corresponds to $\pm$ 2.5 times our Λ mass resolution.

In this way a total of 7336 Λ pairs were selected after verifying that they do not have a track in common. These were grouped into the three di–hyperon samples given in Table 1. The corresponding numbers of Monte Carlo Λ pairs that passed our selection criteria are also shown. Good agreement is seen between the composition of the Monte Carlo generated sample and the data.

Due to the fact that the initial e^+e^- system is an eigenstate of the charge conjugation operator, the inclusive properties of the $\Lambda\Lambda$ and the $\bar{\Lambda}\bar{\Lambda}$ samples should be identical. Experimentally this is not exactly the case since the Λ and $\bar{\Lambda}$ and their decay products have different reaction cross sections with the LEP beam pipe and the OPAL detector materials. In fact, the number of selected $\bar{\Lambda}\bar{\Lambda}$ pairs is

	Data		Monte Carlo	
Sample	No. of pairs	Fraction	No. of pairs	Fraction
$\Lambda\bar{\Lambda}$	5255	71.6%	9628	71.9%
$\Lambda\Lambda$	1095	15.0%	2037	15.2%
$\bar{\Lambda}\bar{\Lambda}$	986	13.4%	1735	12.9%
$(\Lambda\Lambda + \bar{\Lambda}\bar{\Lambda})$	(2081)	(28.4%)	(3771)	(28.1%)
Total	7336	100%	13399	100%

Table 1: *The total number of data and Monte Carlo selected Λ pairs.*

smaller by about 11% than that of the $\Lambda\Lambda$ pairs. In every step of the analysis, where for physics reasons we added these two samples together, we first ascertained that apart from the obvious reduction in the number of $\bar{\Lambda}$ pairs, the two samples behaved similarly.

In Fig. 1a the measured invariant mass distributions of the $\Lambda\bar{\Lambda}$ and the combined $\Lambda\Lambda$ and $\bar{\Lambda}\bar{\Lambda}$ sample are shown. In the $\Lambda\bar{\Lambda}$ distribution a broad low mass enhancement is seen, which in various fragmentation models is associated with local baryon number conservation [1, 8]. No other significant resonance signal is seen[3] in the mass range from 4 to 12 GeV.

The distributions of the $\Lambda\bar{\Lambda}$ and the combined $\Lambda\Lambda$ and $\bar{\Lambda}\bar{\Lambda}$ samples are shown in Fig. 1b as a function of the Q variable used in our analysis. As can be seen, above Q = 4 GeV the two distributions essentially coincide, whereas below 4 GeV the $\Lambda\bar{\Lambda}$ distribution rises due to the correlated production in the hadronisation process.

To exclude from the analysis Λ's that contain a primary s-quark from $Z^0 \to s\bar{s}$ decays, we required that the relative energy $x_E \equiv E_\Lambda/E_{beam}$ was less than 0.3 following reference [18]. This amounted to about 2 % of our data, too small for a meaningful spin correlation analysis.

3.3 Background

The fraction of background (f_{BG}) in our samples was estimated from the data. We considered the two-dimensional data invariant mass distribution of $M(p_1\pi_1)$ versus $M(p_2\pi_2)$. Combinations in which

[3] We estimate that from the decay chain $Z^0 \to J/\psi X; J/\psi \to \Lambda\bar{\Lambda}$ at most five events should contribute to our $\Lambda\bar{\Lambda}$ sample.

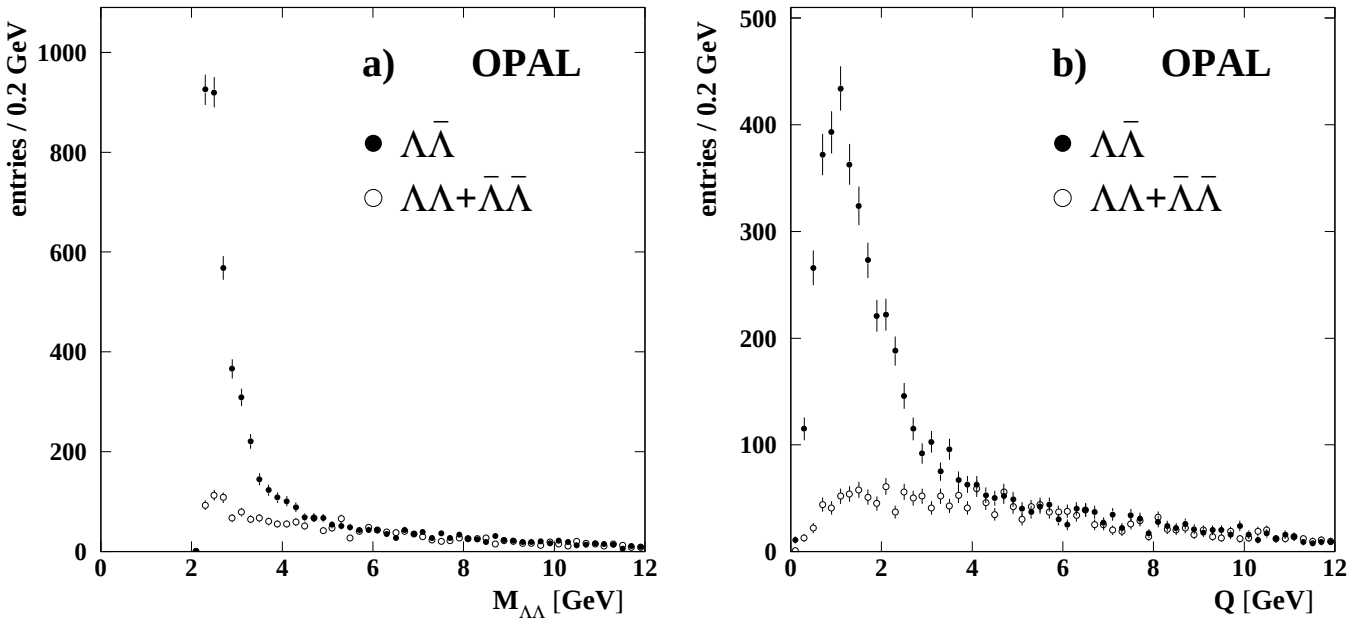

Figure 1: *The invariant mass and Q distributions of the $\Lambda\bar{\Lambda}$ and the combined $\Lambda\Lambda+\bar{\Lambda}\bar{\Lambda}$ data samples.*

both $M(p_1\pi_1)$ and $M(p_2\pi_2)$ fell inside the $\pm$ 6 MeV Λ signal region were the pairs used in our spin composition analysis. The background was then determined by the pairs which fell outside the signal region, as described in Ref. [7]. As a check the background was also investigated with the JETSET Monte Carlo generated sample.

The fraction f_{BG} and its dependence on Q, as obtained from the data and the Monte Carlo, are shown in Fig. 2 for the $\Lambda\bar{\Lambda}$ and for the combined $\Lambda\Lambda$ and $\bar{\Lambda}\bar{\Lambda}$ samples. The purity of the $\Lambda\bar{\Lambda}$ sample below $Q = 2.5$ GeV is constant within errors, having a value of about 90%. This is not the case for the identical hyperon pair samples, where the purity decreases as Q decreases, reaching a level of only about 35% at low Q values. The low statistics at $Q < 0.5$ GeV, together with the low purity of the sample, do not allow a significant measurement of the spin composition of the identical hyperons at this low Q region.

4 Spin Composition Measurements

To measure the spin composition according to the method outlined in Section 2, we performed two Lorentz transformations on each hyperon pair and its decay protons:

1. a transformation from the laboratory system to the di–hyperon CM system, followed by
2. a transformation of each proton momentum to its parent hyperon rest frame.

After these transformations, y^*, the cosine of the angle between the momentum vectors of the decay protons, was calculated. The resolution of y^* is about 0.05, as determined from Monte Carlo studies. In order to account for background effects in our spin composition measurements, we initially modified Eq. 3 to read

$$dN/dy^* = (1 - f_{BG}) \cdot \{(1 - \epsilon) \cdot dN/dy^*|_{S=0} + \epsilon \cdot dN/dy^*|_{S=1}\} + f_{BG} \cdot (1 + \delta \cdot y^*) \qquad (4)$$

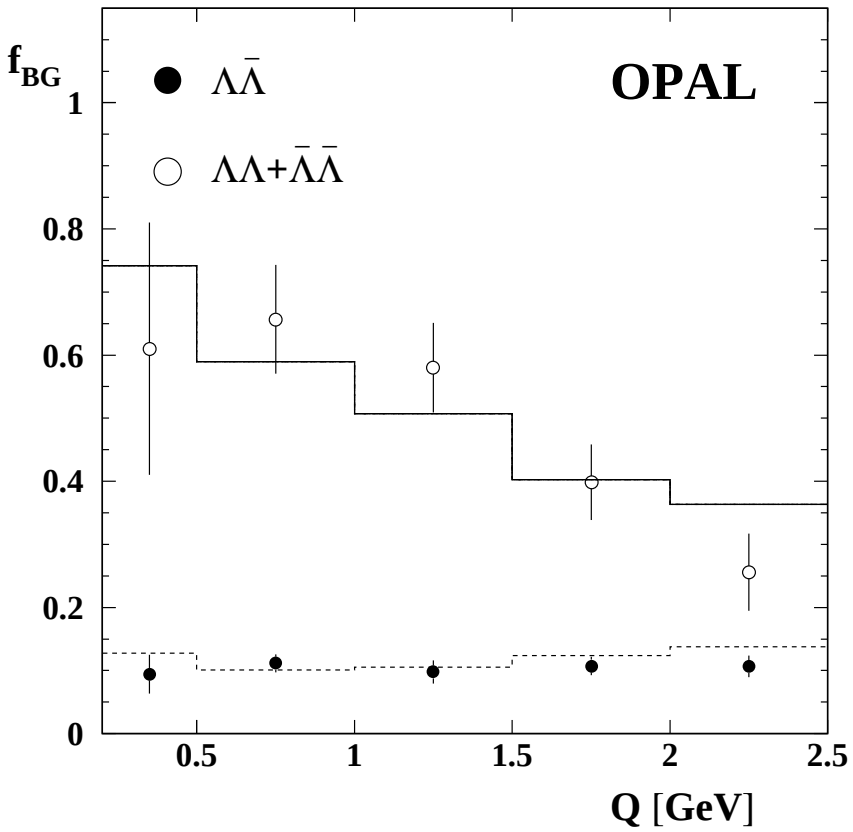

Figure 2: *The background fraction, f_{BG}, plotted as a function of Q for the di–Λ samples as obtained from the OPAL measured data (points with error bars) and from the Monte Carlo studies (lined histograms). The $\Lambda\Lambda$ ($\bar{\Lambda}\bar{\Lambda}$) data below $Q = 0.5$ GeV is not used in the analysis. The error bars represent the statistical and systematic errors added in quadrature.*

where the background fraction f_{BG} is allowed to have a linear y^* dependence with a slope δ. In a systematic study of the background derived from the OPAL data and the Monte Carlo samples, no deviations from a constant y^* behaviour were found over the whole angular range so that the slope parameter δ could be set to zero. Thus Eq. 4 was simplified to:

$$dN/dy^* = (1 - f_{BG}) \cdot \{(1 - \epsilon) \cdot dN/dy^*|_{S=0} + \epsilon \cdot dN/dy^*|_{S=1}\} + f_{BG} \quad (5)$$

For the spin analysis we have divided the data into five Q regions within the range of 0.2 to 2.5 GeV as specified in Table 2.

$\Lambda\bar{\Lambda}$ Data Sample

Q Range (GeV)	0.2 – 0.5	0.5 – 1.0	1.0 – 1.5	1.5 – 2.0	2.0 – 2.5	0.2 – 2.5
$< Q >$ (GeV)	0.39	0.76	1.24	1.73	2.23	1.29
No. of pairs	223	894	928	591	452	3088
f_{BG} (%)	9.1	11.1	9.8	10.7	10.7	10.4
ϵ	0.81	0.69	0.77	0.63	0.67	0.71
$\Delta\epsilon$ (stat)	0.21	0.12	0.11	0.14	0.16	0.06
$\Delta\epsilon$ (syst)	0.03	0.04	0.03	0.04	0.04	0.03

Combined $\Lambda\Lambda$ and $\bar{\Lambda}\bar{\Lambda}$ Data Sample

Q Range (GeV)	0.2 – 0.5	0.5 – 1.0	1.0 – 1.5	1.5 – 2.0	2.0 – 2.5	0.5 – 2.5
$< Q >$ (GeV)	–	0.77	1.25	1.72	2.24	1.53
No. of pairs	–	99	131	124	123	477
f_{BG} (%)	–	65.7	58.0	39.8	25.6	46.2
ϵ	–	– 0.59	0.88	0.72	0.93	0.67
$\Delta\epsilon$ (stat)	–	0.90	0.62	0.46	0.36	0.26
$\Delta\epsilon$ (syst)	–	0.48	0.11	0.05	0.04	0.10

Table 2: *Final results for the fraction of the $S = 1$ contribution to the $\Lambda\bar{\Lambda}$ pairs sample and to the combined $\Lambda\Lambda$ and $\bar{\Lambda}\bar{\Lambda}$ sample in five Q regions as obtained from the maximum likelihood fits of the parameter ϵ. Fit results are also shown for the entire Q range. The statistical errors are those given by the fits.*

To obtain the value of ϵ we have fitted Eq. 5, in each Q range, event by event using the maximum likelihood method. The experimental dN/dy^* distributions are shown in Fig. 3 together with the fitted angular distributions. The ϵ values obtained from the fits and their errors, together with the number of data pairs and their background fractions, are presented in Table 2 for the five chosen Q intervals. The dominant sources of systematic errors are the uncertainties of the background levels and the slope of their y^* distributions. To evaluate these we have repeated the procedure described in section 3.3 varying the position of the areas outside the di–Λ signal region which were used to estimate f_{BG}. The systematic error due to the uncertainties of the δ slope value were estimated by varying the δ values by $\pm\Delta\delta$ given by the fits to the Monte Carlo y^* distributions. We checked that our spin composition results are stable, within the statistical errors, when the mass window cut applied to the M(pπ) distribution was varied between $\pm$ 5 to $\pm$ 10 MeV and so verified that this contribution to the systematic errors was negligible. Finally we have included in the systematic error the uncertainty on the world average value of α_Λ used in Eqs. 1 and 2. The individual contributions to the systematic error on ϵ and their sum in quadrature, $\Delta\epsilon$ (syst), are given in Table 3.

In Fig. 4 we present our final results for the spin composition as a function of Q, with ϵ representing the relative contribution of the S = 1 state. The full circles are the results for the $\Lambda\bar{\Lambda}$ sample and the

$\Lambda\bar{\Lambda}$ Data Sample

	Q Range (GeV)					
Source	0.2 – 0.5	0.5 – 1.0	1.0 – 1.5	1.5 – 2.0	2.0 – 2.5	0.2 – 2.5
f_{BG}	0.002	0.001	0.001	0.002	0.002	0.001
slope δ	0.034	0.035	0.034	0.034	0.034	0.034
α_Λ	0.003	0.003	0.001	0.005	0.004	0.002
$\Delta\epsilon$ (syst)	0.034	0.035	0.034	0.035	0.035	0.034

Combined $\Lambda\Lambda$ and $\bar{\Lambda}\bar{\Lambda}$ Data Sample

	Q Range (GeV)					
Source	0.2 – 0.5	0.5 – 1.0	1.0 – 1.5	1.5 – 2.0	2.0 – 2.5	0.5 – 2.5
f_{BG}	—	0.448	0.027	0.003	0.016	0.018
slope δ	—	0.173	0.102	0.052	0.041	0.103
α_Λ	—	0.056	0.006	0.001	0.008	0.006
$\Delta\epsilon$ (syst)	—	0.483	0.106	0.052	0.045	0.104

Table 3: *The ϵ systematic uncertainties and their sources. These are added in quadrature to obtain $\Delta\epsilon$ (syst), the overall systematic error.*

open circles are for the combined $\Lambda\Lambda$ and $\bar{\Lambda}\bar{\Lambda}$ sample. The error bars represent the statistical errors added in quadrature with the systematic uncertainties. In the Q range of 1.0 to 2.5 GeV the spin composition of both samples is dominated by the S = 1 spin state and is consistent with the value of ϵ = 0.75 which is also the value expected for a statistical spin mixture. In the low Q region of less than 1.0 GeV, the spin composition of the $\Lambda\bar{\Lambda}$ remains the same as at higher Q values, namely $\epsilon \approx 0.75$ whereas the ϵ value of the identical hyperon pair sample is seen to decrease but is still consistent within its error with a statistical spin mixture.

If at low Q values the s-wave ($\ell = 0$) is dominant due to the angular momentum barrier, the ϵ of the combined $\Lambda\Lambda$ and $\bar{\Lambda}\bar{\Lambda}$ sample should approach zero due to the Pauli exclusion principle. This may allow the emitter dimension of the identical $\Lambda\Lambda$ ($\bar{\Lambda}\bar{\Lambda}$) pairs to be extracted. To this end we assume that at high Q values ϵ approaches, from below, the value of 0.75 as expected for a statistical spin mixture. This value is also consistent within errors with our experimental findings. To describe the rise of the S = 0 contribution, given here by $1 - \epsilon$, as Q approaches zero, we have adopted the Goldhaber parametrisation [19] which describes the Bose-Einstein correlation enhancement. Thus the function to be fitted is the one given in Eq. 5 with a Q dependence of ϵ given by:

$$\epsilon(Q) \;=\; 0.75 \cdot (1 \;-\; e^{-Q^2 R_{\Lambda\Lambda}^2}) \tag{6}$$

Here $R_{\Lambda\Lambda}$, the free parameter to be fitted, may be taken as a measure of the size of the identical di–baryon emitter region in analogy to its role in the BEC studies. In this way one is able to carry out a fit over the whole Q range from 0.5 to 2.5 GeV avoiding the need for binning. An unbinned maximum likelihood fit of $R_{\Lambda\Lambda}$ to the data has been performed, with the result of $R_{\Lambda\Lambda} = 0.19\ ^{+0.37}_{-0.07}$ fm, where the errors are taken from the fit. The systematic error is at the level of 0.02 fm. However, $R_{\Lambda\Lambda}$ is consistent with infinity at the level of 1.2 standard deviations[4]. The result of the fit is shown in Fig. 4 by the dashed line.

[4]More than one standard deviation above the fitted $R_{\Lambda\Lambda}$ value the likelihood function does not follow a Gaussian distribution but reaches a plateau.

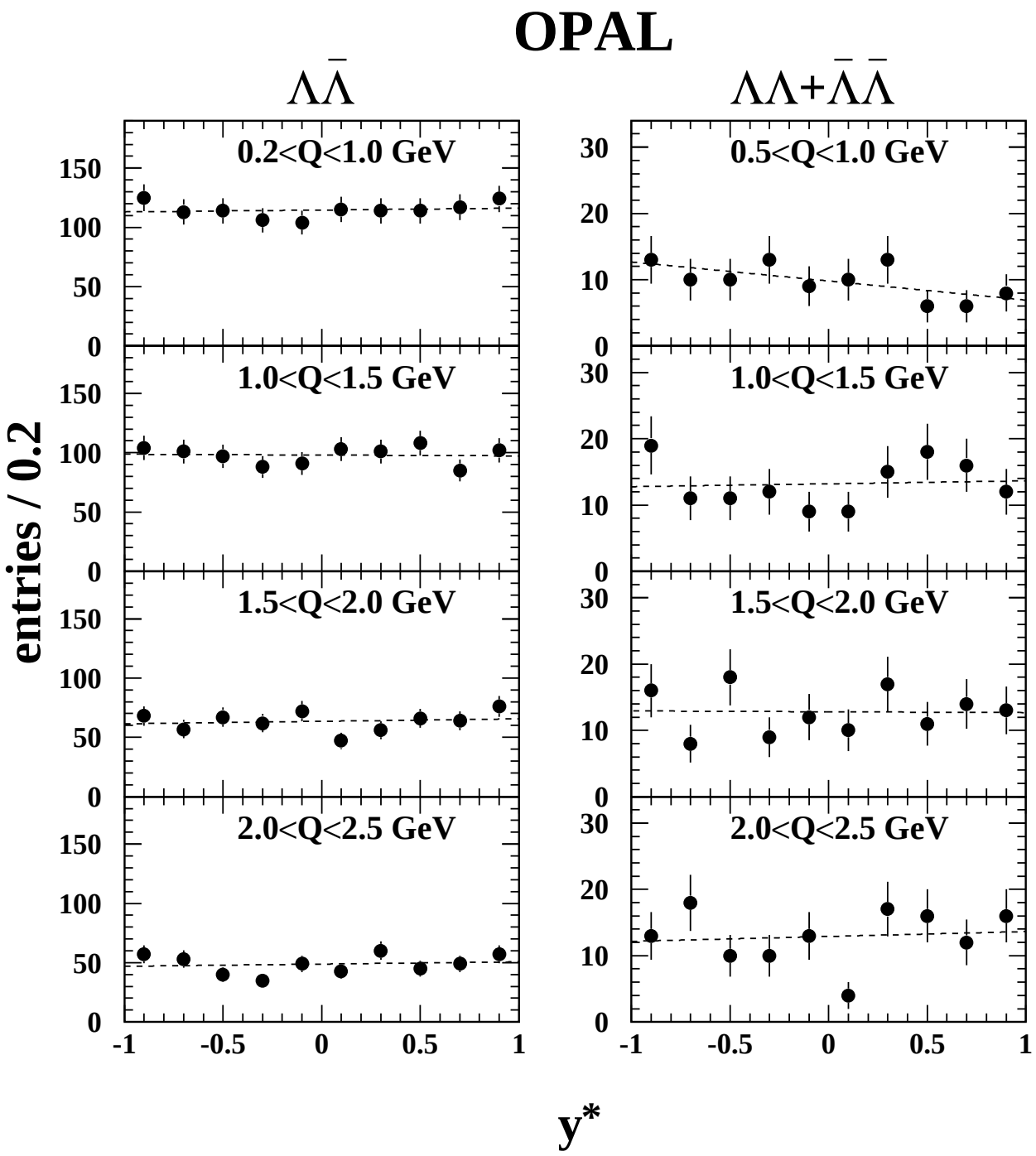

Figure 3: *The measured y^* distributions obtained from the $\Lambda\bar{\Lambda}$ and from the combined $\Lambda\Lambda$ and $\bar{\Lambda}\bar{\Lambda}$ data samples. The dashed lines represent the results of an unbinned maximum likelihood fit (see Table 2).*

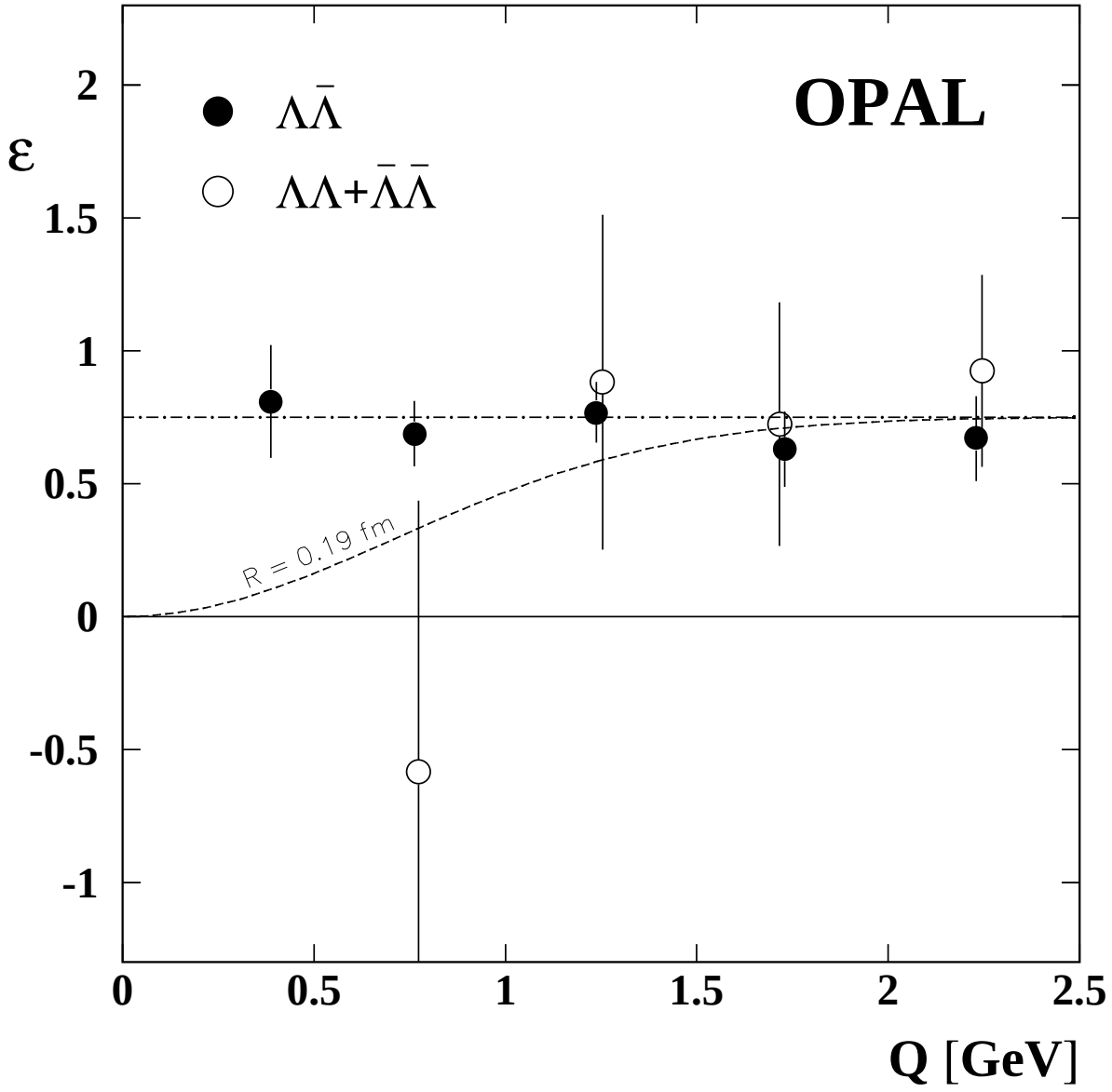

Figure 4: *The measured fraction ϵ of the $S = 1$ state contributions to the di–Λ systems as a function of Q. The full circles are for the $\Lambda\bar{\Lambda}$ sample, and the open circles are for the combined $\Lambda\Lambda$ and $\bar{\Lambda}\bar{\Lambda}$ sample. The error bars represent the statistical and systematic errors added in quadrature. The $\epsilon = 0.75$ dot-dashed line represents the statistical spin distribution. The dashed line describes the Pauli exclusion effect for an emitter radius of 0.19 fm obtained in an unbinned maximum likelihood fit to the combined $\Lambda\Lambda$ and $\bar{\Lambda}\bar{\Lambda}$ sample (see text).*

5 Summary and Conclusions

A first measurement of the spin composition of $\Lambda\bar{\Lambda}$, $\Lambda\Lambda$ and $\bar{\Lambda}\bar{\Lambda}$ pairs in high energy reactions has been carried out in the fragmentation region of the Z^0 multihadron decays. We have used a recently proposed method which is independent of the relative di–Λ angular momentum. Since this method is only valid as long as the energies of the Λ's are non-relativistic in their overall CM system, the analysis was restricted to the region of $Q \leq 2.5$ GeV. The lower Q limits used in our spin analysis were dictated by the statistics and purity of the samples. These limits were set to 0.2 GeV for the $\Lambda\bar{\Lambda}$ sample and to 0.5 GeV for the $\Lambda\Lambda$ and $\bar{\Lambda}\bar{\Lambda}$ data. In our spin analysis, which is model independent, we have used as much as possible the OPAL data to evaluate the purity of our samples and the effects of the background on our measurements.

Over the entire Q range analysed, no significant contribution from resonance decays into a $\Lambda\bar{\Lambda}$ pair is seen, although there is a broad threshold enhancement in the region of $0.5 < Q < 1.5$ GeV. In various fragmentation models this enhancement is accounted for by assuming local baryon number compensation. This interpretation is supported by our spin measurement in this enhancement region for which we obtain $\epsilon = 0.73 \pm 0.08 \pm 0.04$, indicating that the S = 0 and the S = 1 states contribute with a relative strength proportional to 2S + 1.

No evidence for exotic di–baryon resonances is seen in our combined $\Lambda\Lambda$ and $\bar{\Lambda}\bar{\Lambda}$ mass distribution above $Q = 1.0$ GeV. The errors of our spin measurements are too large to detect any region which is clearly a single spin state. The Q region below 0.5 GeV, where the $\Lambda\Lambda$ resonance state referred to as the H particle [20] is most likely to be present, is inaccessible to us due to insufficient statistics and low Λ purity. In the Q region between 0.5 and 1.0 GeV, the S = 1 contribution is found to be consistent with zero, associated however with a large error so that a statistical mixture cannot be excluded. If this behaviour is attributed to the Pauli exclusion principle, then it can be associated with an emitter radius of $R_{\Lambda\Lambda} = 0.19\ ^{+0.37}_{-0.07}$ fm. It is however consistent with infinity within 1.2 standard deviations.

Apart from this single low ϵ value, the spin composition over the whole analysed Q region, of both the $\Lambda\bar{\Lambda}$ and the identical hyperon pairs $\Lambda\Lambda$ and $\bar{\Lambda}\bar{\Lambda}$ is dominated by the S = 1 state having a contribution of about 75%. Summing up all the $\Lambda\bar{\Lambda}$ data one obtains the value $\epsilon = 0.71 \pm 0.06 \pm 0.03$ which is more than 4 standard deviations away from a pure S = 1 state. For the identical hyperons the corresponding result averaged over the $0.5 < Q < 2.5$ GeV range is $\epsilon = 0.67 \pm 0.26 \pm 0.10$.

If the properties of $\Lambda\bar{\Lambda}$ pairs produced in Z^0 decays are dominated by the vector nature of a single gluon, the state $S_{\Lambda\bar{\Lambda}} = 1$ should predominate and yield $\epsilon \approx 1$. Due to the fact that an isolated gluon cannot produce a colourless $\Lambda\bar{\Lambda}$ pair, a reduction in the contribution of the S = 1 state can occur during the colour fading process mediated by soft gluon emission. Thus in the absence of reliable QCD calculations, a value of $\epsilon = 0.75$ from this process cannot yet be ruled out. However, the observation that ϵ for the $\Lambda\bar{\Lambda}$ pairs is consistent with the value 0.75 over the whole analysed Q range, as also for the identical Λ hyperons at Q above 1.0 GeV, strongly suggests that the spin compositions of all di–Λ samples are as expected from a statistical spin distribution, representing an average over many allowed QCD production processes and baryons' decay.

Acknowledgements

We thank J. Ellis, K. Kinder-Geiger and H.J. Lipkin for many helpful discussions concerning the theoretical aspects of this work. It is a pleasure to thank the SL Division for their efficient operation of the LEP accelerator and for their continuing close cooperation with our experimental group. In

addition to the support staff at our own institutions we are pleased to acknowledge the
Department of Energy, USA,
National Science Foundation, USA,
Particle Physics and Astronomy Research Council, UK,
Natural Sciences and Engineering Research Council, Canada,
Israel Ministry of Science,
Israel Science Foundation, administered by the Israel Academy of Science and Humanities,
Minerva Gesellschaft,
Japanese Ministry of Education, Science and Culture (the Monbusho) and a grant under the Monbusho International Science Research Program,
German Israeli Bi-national Science Foundation (GIF),
Direction des Sciences de la Matière du Commissariat à l'Energie Atomique, France,
Bundesministerium für Bildung, Wissenschaft, Forschung und Technologie, Germany,
National Research Council of Canada,
Hungarian Foundation for Scientific Research, OTKA T-016660, and OTKA F-015089.

References

[1] For a recent review see e.g., B.R. Webber, *Hadronization*, Cavendish-HEP-94/17, Lectures given at the Summer School on Hadronic Aspects of Collider Physics, Zuoz, Switzerland, August 1994.

[2] J. Ellis and K. Geiger, Phys. Rev. **D52** (1995) 1500, and CERN-TH-95-283 (to be published).

[3] B. Andersson, *Bose Einstein Correlation in the Lund Model*, Lund university preprint LUTP 95-33, Proc. of the XXV Multiparticle Dynamics Symposium, 1995 (in print).

[4] M. Cacciari and M. Greco, Phys. Rev. Lett. **73** (1994) 1586;
M. Cacciari et. al., Phys. Lett. **B356** (1995) 553;
P. Cho, A.K. Leibovich, Phys. Rev. **D53** (1996) 150;
K. Cheung, W.Y. Keung, T.C. Yuan, Phys. Rev. Lett. **76** (1996) 87, and references therein.

[5] B. Andersson, G. Gustafson and T. Sjöstrand, Physica Scripta **32** (1985) 574.

[6] G. Alexander and H.J. Lipkin, Phys. Lett. **B352** (1995) 162.

[7] OPAL Collab., P. Acton et al., Phys. Lett. **B291** (1992) 503.

[8] T. Sjöstrand, Comp. Phys. Comm. **39** (1986) 347;
T. Sjöstrand and M. Bengtsson, Comp. Phys. Comm. **43** (1987) 367;
T. Sjöstrand, Comp. Phys. Comm. **82** (1994) 74.

[9] J. Allison et al., Nucl. Inst. and Meth. **A317** (1992) 47.

[10] OPAL Collab., P. Acton et al., Z. Phys. **C58** (1993) 387;
OPAL Collab., G. Alexander et al., Z. Phys. **C69** (1996) 543.

[11] See for example E. Segrè, *Nuclei and Particles*, 2nd Edition (Benjamin/Cummings Publishing Co.), p. 876.

[12] E.P. Wigner, Z. Phys. **43** (1927) 624;
C. Eckart, Rev. Mod. Phys. **2** (1930) 305.

[13] L. Montanet et al., *Review of Particle Properties*, Phys. Rev. **D50** part I, (1994) 1173.

[14] OPAL Collab., K. Ahmet et al., Nucl. Instr. and Meth. **A305** (1991) 275;
P. P. Allport et al., Nucl. Instr. Meth. **A324** (1993) 34;
P. P. Allport et al., Nucl. Instr. Meth. **A346** (1994) 476.

[15] M. Hauschild et al., Nucl. Instr. and Meth. **A314** (1992) 74.

[16] O. Biebel et al., Nucl. Instr. and Meth. **A323** (1992) 169.

[17] OPAL Collab., G. Alexander et al., Z. Phys. **C52** (1991) 175.

[18] G. Gustafson, J. Häkkinen, Phys. Lett. **B303** (1993) 350.

[19] G. Goldhaber et al., Phys. Rev. Lett. **3** (1959) 181, and Phys. Rev. Lett. **120** (1960) 300.

[20] First suggested by R.L. Jaffe, Phys. Rev. Lett. **38** (1977) 195. For more recent accounts see e.g., J.L. Ping in Proc. of the XIII Int. Conf. on Particles and Nuclei, 28 June – 2 July 1993, Perugia, Italy, p. 526; ibid. S. Paul p. 646.